Neural Processing Letters (2022) 54:3489–3505
https://doi.org/10.1007/s11063-022-10775-z

Iris Recognition using Multi Objective Artificial Bee Colony Optimization Algorithm with Autoencoder Classifier

Sheela S V[1] · **Radhika K R**[1]

Accepted: 6 February 2022 / Published online: 15 March 2022

Abstract
In recent decades, iris recognition is a trustworthy and important biometric model for human recognition. Criminal to commercial products, citizen confirmation and border control are few application areas. The research work is a deep learning based integrated model for accurate iris detection and recognition. Initially, eye images are considered from two datasets, the Chinese Academy of Sciences Institute of Automation (CASIA) and the Indian Institute of Technology (IIT) Delhi v1.0. Iris region is accurately segmented using Daugman's algorithm and Circular Hough Transform (CHT). Feature extraction is hybrid that is performed using Dual Tree Complex Wavelet Transform (DTCWT), Gabor filter, Local Binary Pattern (LBP) and Gray Level Co-occurrence Matrix (GLCM) from the segmented iris regions. A Multiobjective Artificial Bee Colony (MABC) algorithm is proposed to eliminate noisy and redundant feature vectors by estimating consistent information. In MABC algorithm, two multi-objective functions are formulated as reduction in number of features and classification error rate. The selected active feature vectors are given as input to autoencoder classification for iris recognition. The experimental outcome shows that MABC-autoencoder model obtained 99.67% and 98.73% accuracy on CASIA-Iris, and IIT Delhi v1.0 iris datasets. Performance evaluation is based on accuracy, specificity, Critical Success Index (CSI), sensitivity, Fowlkes Mallows (FM) index, and Mathews Correlation Coefficient (MCC).

Keywords Autoencoder · Circular Hough transform · Daugman's algorithm · Iris recognition · Local binary pattern · Multi objective artificial bee colony

1 Introduction

Pattern recognition is observed to be the most emerging research area, which can obviate issues in different aspects. In current scenario, numerous methods are used for authentication such as password, signature and identification cards, which can be easily faked, stolen or lost [1, 2]. Biometric features like face, iris, fingerprint, hand and finger vein play an

Sheela S V

[1] Dept. of Information Science and Engineering, BMS College of Engineering, Bangalore, India

important role in user authentication, which are considered more reliable and secure, especially in personal identification [3, 4]. Applications of biometric recognition are observed in finance, banking, public safety, immigration, attendance management, border controls, and healthcare [5]. Iris recognition is found to be a reliable and efficient method for human identification due to its invariant and unique features [6]. The factors that play an important role in increasing the attention of iris recognition are unique pattern, user-friendly image acquisition devices and permanence structure [7].

Iris is a thin eye structure, which consists of abundant eye characteristics that create secure authentication. Rich texture patterns are immutable, and invariant as compared to other biometrics like speech, fingerprint and face [8, 9]. In recent times, many automated models are developed by researchers using iris features for secure authentication [10]. Computation time and accuracy are crucial factors to analyze iris recognition system [11]. The work aims to enhance iris recognition performance by applying a deep learning classifier with multi-objective optimizer.

The paper is structured as follows. The objectives are represented in Sect. 2. The state-of-art literature is discussed in Sect. 3. Description of MABC-autoencoder model is enumerated in Sect. 4. The quantitative and comparative evaluation of MABC-autoencoder model is depicted in Sect. 5, and the conclusion is provided in Sect. 6.

2 Objectives

In the present work, a novel deep learning based integrated model is proposed for precise iris recognition. The objectives are listed below:

- Accurate segmentation of iris region using CHT and Daugman's algorithm. CHT segments pupil and sclera boundaries from the eye images, and Daugman's algorithm converts iris circular region into a rectangular region that corrects the pupil displacement.
- Hybrid feature extraction using DTCWT, Gabor filter, LBP and GLCM. Feature vectors are extracted from segmented iris regions.
- Implementation of MABC algorithm reduces the size of extracted feature vectors by selecting discriminative or active feature vectors that decrease execution time, and complexity of the model.
- Development of autoencoder classification based on discriminative feature vectors for iris recognition. In this scenario, the MABC-autoencoder model performance is analyzed based on accuracy, specificity, CSI, sensitivity, FM index, and MCC.

3 Related work

Dua et al. used Hough transform and integrodifferential operator to segment iris sclera and pupil-iris boundaries from acquired images [12]. Image normalization was accomplished using Daugman's rubber sheet model to convert iris circular region into rectangular region. One dimensional Gabor filtering was applied to extract feature vectors from the segmented regions. Classification was performed by Radial Basis Function Neural Network (RBFNN), and Feed Forward Neural Network (FFNN) to classify authorized individuals. Nithya and Lakshmi combined first and second order statistical measures for extracting texture feature values from raw eye images [13]. A hybrid statistical dependency based feature selection method was developed to reduce the size of extracted features by removing redundant and noisy feature vectors. Neural network with Levenberg Marquardt training technique was implemented for iris recognition. Ahmadi et al. presented iris recognition model based on polynomial filter, step filter and two dimensional Gabor kernel for pre-processing and feature extraction [14]. RBFNN with a genetic algorithm was used for iris matching to authorize respective individuals. The extensive experimental analysis confirmed that the presented model obtained better performance in iris recognition by means of execution time and accuracy.

In continuum, Ahmadi and Akbarizadeh presented iris recognition model based on particle swarm optimizer and multilayer perceptron neural network [15]. An extensive experiment confirmed that the presented model achieved good recognition performance. Adamović et al. initially used Daugman's approach for iris localization and normalization, and then base64 encoder was applied to transform normalized image into text without affecting statistical characteristics [16]. After image transformation, language-independent feature vectors were extracted and finally template matching was accomplished with an optimal set of feature vectors using random forest classification technique. Shuai et al. developed a novel framework for multi-state heterogeneous iris recognition [17]. Initially, Convolutional Neural Network (CNN) was used in pre-processing phase to convert the eye images into recognition labels. Multi-source feature fusion process and statistical learning ideas were utilized for iris recognition. Chen, et al. introduced a new feature extraction technique for reasonable iris recognition [18]. The developed Tiger center (T-center) loss function was utilized to reduce the problems generated due to insufficient discrimination in conventional softmax loss function. T-center loss function significantly enhanced the discriminative power of deep features based on CNNs. The extensive experiment showed that the developed T-center loss function improves effectiveness of iris recognition on large-scale iris samples and cross datasets.

Tobji, et al. presented an algorithm named FMnet for heterogeneous iris recognition [19]. The FMnet algorithm was developed based on Multi-scale CNN (MCNN) and Fully Convolutional Network (FCN), where it obtained acceptable recognition performance at different image resolutions. The experimental investigation showed that FMnet algorithm achieved better classification results compared to traditional recognition algorithms. Jayanthi, et al. introduced a novel model for iris recognition that contains four stages; image pre-processing, region detection, segmentation and recognition [20]. At first, Gamma correction, black hat filter and median filter were applied to pre-process eye images. Further, a Hough Circle Transform (HCT) was applied to localize the region of interest, and Region proposal network with CNN (R-CNN) by Inception v2 model was employed for iris recognition. Vyas, et al. presented a feature extraction technique based on polynomial fitting and curvelet transform [21]. In the transform, the developed feature descriptor uses wedge shaped sub-bands for covering the frequency spectrum to characterize images. In addition, a two dimensional polynomial fitting was applied on the curvelet sub-bands to generate complete feature vector. The experimental investigation showed the eminence of developed feature descriptor, which was progressive in iris recognition compared to recent and standard techniques.

Juneja and Rana, developed a hybrid model using kernel principal component analysis with Gabor features to precisely recognize the eye images [22]. The simulation result demonstrated that hybrid model reduced error rate, and improved recognition accuracy related to the traditional models. Kumar and Arthi, introduced a Hierarchical Collaborative Representation based Classification (HCRC) technique for iris recognition [23]. The HCRC technique included four phases; (i) hybrid median filter to denoise collected images, (ii) threshold based segmentation and geodesic region based active contour level set methods for segmentation, (iii) feature vectors extraction using local ternary pattern, and (iv) iris recognition. Jan and Min-Allah, introduced an optimized coarse to fine method for marking the inner, and outer iris boundaries [24]. Fourier series was utilized to mark reflections and eyelids in polar form and to regularize non-circular iris contour. Jan, et al. utilized geometry and centroid concepts to extract pupil's radius and center from the collected eye images [25]. Fourier series and CHT were used to refine coarse iris boundaries and to mark iris outer boundaries. The experimental result confirmed that presented model achieved substantial performance in iris recognition related to traditional models. Existing literature address three major issues in iris recognition; occlusion, motion blur, and defocus. The system with fixed focus optic lens generates defocused eye images, and the iris scanners work only in closer range with stationary targets, where it is inappropriate to record eye images from moving target [26]. In addition, longer processing time for authentication, complexity in recognition, reduced true positive rate and lack of accurate recognition rate are traditional concerns in iris recognition [27].

The contemporary work has paved a way to propose an innovative model working with minimum discriminant feature vectors to enhance iris recognition performance. Implementation of MABC feature selection and autoencoder model showed further improvement.

4 Methodology

The proposed iris recognition model includes five phases, **image collection, segmentation, feature extraction, selection and classification.** The model is represented in Fig. 1.

4.1 Image collection

Various algorithms in existing literature have adopted benchmark datasets for experimentation. On similar basis, the proposed MABC-autoencoder model is investigated on two benchmark datasets: IIT Delhi v1.0 iris dataset and CASIA-Iris dataset. The eye images are high resolution that help in capturing more eye details for enhanced recognition. The

Fig. 1 Proposed model

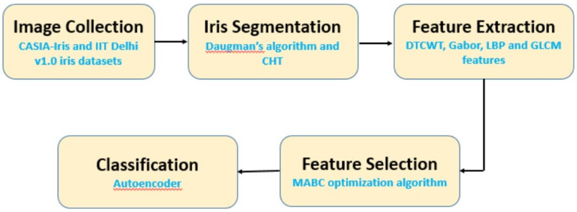
Image Collection
CASIA-Iris and IIT Delhi v1.0 iris datasets
Iris Segmentation
Daugman's algorithm and CHT
Feature Extraction
DTCWT, Gabor, LBP and GLCM features
Feature Selection
MABC optimization algorithm
Classification
Autoencoder

IIT Delhi v1.0 iris dataset comprises 1120 eye images (896 images for training and 224 images for testing), which are recorded from the staff and students at IIT Delhi, India [28]. The dataset was recorded from January to July 2007 in biometrics research laboratories. In this dataset, eye images are recorded from 224 subjects (48 female subjects, and 176 male subjects) in bitmap format. The images were captured using JIRIS, JPC1000, digital CMOS camera. The sample eye images are provided in Fig. 2.

CASIA-Iris thousand dataset comprises 20,000 eye images (16,000 images for training and 4000 images for testing) that are recorded from 1000 subjects. Eye images are captured using user friendly dual eye iris camera called IKEMB 100 camera [29]. In this dataset, the main sources of intraclass variations are specular reflection and eye-glass. The sample eye images are depicted in Fig. 3.

4.2 Iris Segmentation

Iris segmentation is accomplished using Daugman's algorithm and CHT. Daugman's algorithm is a circular edge detector, which uses integro differential operator to find inner, and outer boundaries of the iris regions, and also significantly defines elliptical boundaries of eyelids. The integro differential operator is mathematically defined in Eq. (1).

$$\max_{(r,x_0,y_0)} \left| G_\sigma(r) \times \frac{\partial}{\partial r} \int_{(r,x_0,y_0)} \frac{a(x,y)}{2\pi r} ds \right| \tag{1}$$

where, $G_\sigma(r)$ represents Gaussian smoothing function along with factorσ, r represents radius to search and $a(x,y)$ indicates images, where eye is in the contour of circle(r, x_0, y_0) . The images scanned have maximum circular arc ds of r and gradient changes with the center coordinates(x_0, y_0). The segmentation process starts with outer boundaries located between iris and white sclera. While σ is fixed, higher contrast is obtained to detect outer boundaries. Daugman's algorithm attained better segmentation performance, even in the presence of eyelids, and eyelashes. Additionally, CHT is used to compute radius and center coordinates between pupil and iris. The radius of image and center coordinates x_c and y_c are computed using $x_c^2 + y_c^2 = r^2$

In this scenario, radius is defined by edge points and center co-ordinate points are defined by the maximum points in Hough space. The inner sclera/iris boundaries are weighted equally to create an edge map using horizontal, and vertical gradients in the Canny edge detection. Initially, CHT is carried out for sclera/iris boundary and then for the pupil/iris

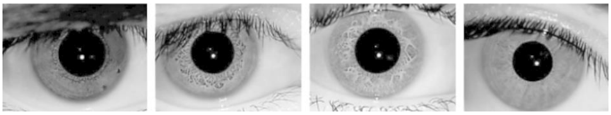

Fig. 2 Sample eye images from IIT Delhi v1.0 iris dataset

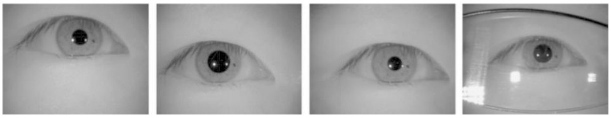

Fig. 3 Sample eye images from CASIA-Iris thousand dataset

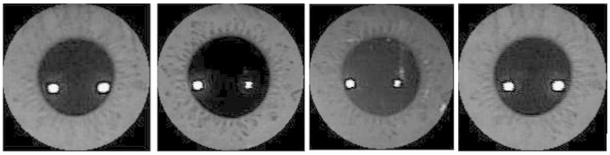

Fig. 4 Segmented output image of Daugman's algorithm and CHT

boundary for an efficient and accurate recognition [12]. The output of Daugman's algorithm and CHT is depicted in Fig. 4.

4.3 Feature extraction and selection

Following precise segmentation of iris region, feature extraction is performed utilizing DTCWT, Gabor, LBP, and GLCM features. DTCWT comprises two parallel decimated trees, and a complex filter to separate adjacent quadrants of two dimensional spectrum. DTCWT has properties like perfect reconstruction, limited computation, good directional selectivity and shift invariance to attain better image recognition. A quad tree structure is generated with four trees such that two trees represent columns, and two trees for rows of the image [30]. In DTCWT, the segmented iris image is decomposed by six complex wavelet functions and a scaling function. In addition, features are computed from the segmented iris images by utilizing Gabor filter bank [31]. The extracted features are highly redundant and multi-dimensional. The feature dimension is reduced using Gabor filter. The filtered Gabor feature vectors are significant in classifying the required data.

The LBP feature descriptor represents image texture by encoding pixel information in a segmented iris image. Every pixel of a segmented iris image is considered as a center pixel, and then LBP features are extracted by comparing the center pixel with the local surrounding pixels [32]. Additionally, a GLCM feature descriptor is applied for computing second order characteristics of segmented iris images [33]. The GLCM feature extraction techniques considered are sum of squares, contrast, correlation, energy, entropy, homogeneity, sum average, sum variance, sum entropy, difference variance, difference entropy and information measure of correlation. This provides relative position of neighborhood pixels in a segmented iris image to yield better recognition. The LBP and GLCM feature descriptors effectively extract texture and color information from the segmented iris images that help in achieving good recognition results. The undertaken feature descriptors such as DTCWT, Gabor, LBP and GLCM extract 10,568 feature vectors. MABC algorithm is used to reduce the dimension of the extracted feature vectors such that the complexity of model is reduced.

The Artificial Bee Colony (ABC) is a robust and simple algorithm, which is developed to solve optimization problems. The algorithm mimics the behavior of honey bees, where artificial bee colonies include three groups of bees: scout bees, onlooker bees, and employed bees. The bees waiting in the search area to decide for selecting food source are named onlooker bees, and the bees that are going to visit food sources are called employed bees [34]. Additionally, scout bees make a random walk in the search area to discover new food sources. In this algorithm, the food source location is considered as a solution to the optimization problems, and the food source amount depends on quality of the related solutions, defined by fitness, where fitness function fit_i is mathematically formulated in Eqs. (3) and (4).

$$fit_i = \frac{1}{1 + b_i} \tag{3}$$

$$b_i = \frac{1}{D_{train}} \sum_{i,j=1}^{D_{train}} d(s_j, w_i^{Cluster_{known}(s_j)}) \tag{4}$$

where, D_{train} denotes number of training patterns, s_j represents location of the patterns, and $w_i = 100$ states initial population size. Further, the onlooker bee selects food source, denoted as discriminative feature vectors based on the probability value related with food sourcee_i, which is defined in Eq. (5) [35].

$$e_i = \frac{fit_i}{\sum_{n=1}^{SN} fit_n} \tag{5}$$

where, fit_i states fitness function and SN represents a number of food sources. To further improve performance of the discriminative feature vector selectiond_f, multi-objective functions are included in the existing ABC algorithm. The multi-objective functions included in ABC optimizer are provided as reduction in features and minimum error rate for classification.

The minimization problem of multi-objective functions are mathematically determined in Eqs. (6), (7), and (8).

$$Function_1\,(x) = \frac{ABC_f}{T_f} \tag{6}$$

$$Function_2\,(x) = \frac{FP + FN}{TP + TN + FP + FN} \times 100 \tag{7}$$

$$d_f = \left\{ \begin{array}{l} Function_1\,(x) \\ Function_2\,(x) \end{array} \right\} \tag{8}$$

where, $Function_1\,(x)$ denotes the ratio of selected features as first objective, $Function_2\,(x)$ states the classification error rate as second objective, ABC_f represents selected features of ABC algorithm, T_f indicates the total extracted features, TP indicates true positive value, FP represents false positive value, TN states true negative value, FN denotes false negative value, and d_f represents the selected discriminative feature vectors. In this work, ABC_f = 5637, T_f= 10,568 and d_f= 3810.

4.4 Classification

In continuum with obtaining the discriminative feature vectorsd_f, iris recognition is carried out by using autoencoder classification technique [36]. The autoencoder is an unsupervised deep learning based classification technique, where the number of hidden nodes is higher compared to the number of input nodes, and number of input nodes is similar to the number of output nodes. As compared to traditional classification techniques, possibility of missing value is limited in autoencoder during iris recognition. The classification technique initially allocates a score to the obtained discriminative feature vectors $f(d_f)$, where f contains a sequence of layers for computation, which are mathematically determined in Eq. (9).

$$Z_{ij} = I_i P_{ij}; Z_j = \sum_{ij} Z_{ij} + h_j; O_j = u\left(Z_j\right) \tag{9}$$

where, $u(Z_j)$ denotes pooling or mapping function, h_j represents hidden layer, O_j denotes output layer, P_{ij} states model parameter, and I_i states input layer. In autoencoder classification technique, the layer wise relevance propagation decomposes $f(d_f)$ into relevance attributel_i, which is stated in equation (10).

$$f(d_f) = \sum\nolimits_i l_i, l_i = \sum_j \frac{zij}{\sum_i zij} \tag{10}$$

The classification decision is supported byl_i, where $l_i > 0$ represents positive evidence and$l_i < 0$ states negative or neutral evidence. During pre-training mechanism, the bias and weight parameters are learned to reduce the cost function that is mathematically determined in equation (11).

$$cost = \frac{1}{2n} \sum_{i=1}^{n} \left(\widehat{I_i} - I_i\right)^2 + \beta \sum_{j=1}^{m} KL\left(p|\widehat{p_j}\right) + \frac{\lambda}{2} \sum_{i=1}^{n} \sum_{j=1}^{m} \theta_{ij}^2 \tag{11}$$

where, λ indicates weight delay, p denotes sparsity parameter, θ states weight of hidden layers, β denotes weight of sparsity penalty, $\widehat{p_j}$ represents probability of firing activity,m denotes hidden nodes, KL represents Kullback-Leibler divergence function and n specifies number of input nodes or input size. The hyper-parameter settings of autoencoder classification technique is indicated as follows: learning rate is 0.1, hidden layer size is 500, epoch is 100, input layer is 1, output layer is 1, L_2 weight regularization is 0.004, sparsity regularization is 4 and sparsity proportion is 0.15. The experimental investigation of proposed MABC-autoencoder model is explained in the next section.

5 Experiment and Results

The proposed MABC-autoencoder model is simulated using MATLAB R2019 software. The effectiveness of model is evaluated by comparing a set of prior models such as fully and multi-scale CNN [19], integrated deep learning model [20], coarse to fine method-Fourier series [24], and CHT-Fourier series [25] on CASIA-Iris dataset and IIT Delhi v1.0 iris dataset. Additionally, the model is validated by six performance measures like accuracy, MCC, specificity, CSI, sensitivity and FM index that are mathematically represented in the Eqs. (12-17).

$$Accuracy = \frac{TP + TN}{TN + TP + FN + FP} \times 100 \tag{12}$$

$$MCC = \frac{TP \times TN - FP \times FN}{\sqrt{(TN + FN)(TN + FP)(TP + FN)(TP + FP)}} \times 100 \tag{13}$$

$$Specificity = \frac{TN}{TN + FP} \times 100 \tag{14}$$

$$CSI = \frac{TP}{TP + FP + FN} \times 100 \tag{15}$$

$$Sensitivity = \frac{TP}{TP + FN} \times 100 \tag{16}$$

Table 1 Performance evaluation of MABC-autoencoder model on IIT Delhi v1.0 iris dataset with different feature extraction and classification techniques

Without feature selection							
Features	*Classifiers*	*Accuracy (%)*	*Sensitivity (%)*	*Specificity (%)*	*MCC (%)*	*CSI (%)*	*FM (%)*
GLCM	KNN	62.96	61.72	46.24	65.34	43.85	55.60
	DT	45.96	60.59	68.63	44.95	60.77	45.50
	RF	58.57	59.93	52.43	40.27	61.40	30.76
	MSVM	66.21	61.47	69.68	69.03	61.84	65.04
	AdaBoost	53.42	61.89	64.96	57.71	58.72	56.51
	Autoencoder	75.13	79.79	80.53	84.80	65.56	80.03
LBP	KNN	53.20	55.39	47.40	53.85	47.42	62.16
	DT	43.48	51.36	69.80	49.12	43.85	50.37
	RF	46.08	49.25	47.21	55.50	48.50	50.76
	MSVM	65.20	67.21	57.88	67.09	62.81	75.49
	AdaBoost	62.65	60.56	55.78	60.99	43.24	61.70
	Autoencoder	76.96	80.16	73.41	79.19	75.08	75.48
Gabor	KNN	64.28	63.78	53.38	65.49	52.17	66.80
	DT	57.52	58.11	72.57	57.58	57.40	57.32
	RF	58.63	62.16	65.12	60.67	60.01	62.13
	MSVM	76.12	73.77	69.81	76.68	63.77	76.96
	AdaBoost	65.35	65.84	67.24	65.26	51.37	66.75
	Autoencoder	86.02	83.52	83.65	86.53	75.97	86.04
DTCWT	KNN	64	63.22	51.64	65.45	51.21	65.74
	DT	56.63	57.22	71.26	55.80	66.37	55.92
	RF	57.50	60.25	63.27	60.63	68.34	60.85
	MSVM	75.63	73.20	69.75	76.43	63.31	76.65
	AdaBoost	65.22	64	65.64	65.19	50.70	65.49
	Autoencoder	84.25	83.44	81.84	85.20	75.53	85.34
Hybrid	KNN	60.59	62.83	81.76	60.92	50.71	66.14
	DT	62.68	60	81.99	63.99	47.58	62.26
	RF	74.74	78.41	83.75	74.37	71.62	80.51
	MSVM	75.09	77.97	86	82.82	88.33	77.96
	AdaBoost	85.85	89.72	90.36	87.70	84.02	88.55
	Autoencoder	92.48	97.06	93.95	92.90	96.18	93.70

$$FMindex = \sqrt{\frac{TP}{TP+FP} \times \frac{TP}{TP+FN}} \times 100 \tag{17}$$

5.1 Quantitative study on IIT Delhi v1.0 iris dataset

MABC-autoencoder model performance is validated on IIT Delhi v1.0 iris dataset, which has 1120 eye images with a resolution of320×240. In this work, 5 fold cross-validation is accomplished for experimental investigation which gives more information about the model performance. With deep learning models, cross validation is a preventative measure against overfitting issues and improves the estimated performance of MABC-autoencoder model.

In Table 1, performance evaluation is realized using distinct feature extraction techniques: GLCM, LBP, DTCWT, Gabor and hybrid features, and classification techniques: Multi Support Vector Machine (MSVM), Random Forest (RF), Decision Tree (DT), K-Nearest Neighbor (KNN), AdaBoost and autoencoder. MSVM performs classification using one-to-one approach by splitting multiclass problem into multiple binary classification problem. With error-correcting output code model, predictions of binary classifiers are aggregated. The classifier uses C(C-1)/2 binary SVM models and radial basis function kernel, where ‘C’ is the number of unique class labels. RF combines results of bootstrap-aggregated (bagged) decision trees to improve generalization and reduce the effect of overfitting. Random subset of predictors are selected at each decision split. DT approach fits binary tree structures for multiclass categorization. KNN determines classification model based on local approximation. Adaboost combines a set of weights over multiple iterations to generate a sequence of hypothesis. Linear combination of weak classifiers are cascaded to construct a strong classifier. Autoencoder does not require labeled data resulting in unsupervised deep neural network model. Training process is based on optimization of cost function to measure the error.

The hybrid features with autoencoder obtained maximum results in iris recognition, which are effective related to comparative classifiers and individual feature extraction techniques in light of accuracy, sensitivity, specificity, MCC, CSI and FM index. As indicated in Table 1, the combination of hybrid features with autoencoder achieved higher accuracy of 92.48%, sensitivity of 97.06%, specificity of 93.95%, MCC of 92.90%, FM index of 93.70%, and CSI of 96.18% in iris recognition on IIT Delhi v1.0 iris dataset. The graphical presentation of proposed model on IIT Delhi v1.0 iris dataset with different feature extraction and classification techniques is stated in Fig. 5.

In Table 2, performance evaluation is accomplished by feature selection techniques like Particle Swarm Optimizer (PSO), Grey Wolf Optimizer (GWO), Ant Colony Optimizer

Fig. 5 Graphical presentation of MABC-autoencoder model on IIT Delhi v1.0 iris dataset with different feature extraction and classification techniques

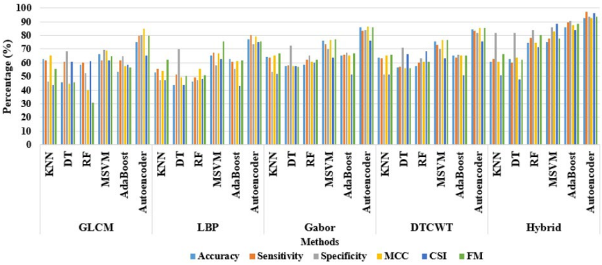

Table 2 Performance evaluation of MABC-autoencoder model on IIT Delhi v1.0 iris dataset with different feature selection algorithms

With feature selection

Optimizers	*Classifiers*	*Accuracy (%)*	*Sensitivity (%)*	*Specificity (%)*	*MCC (%)*	*CSI (%)*	*FM (%)*
PSO	KNN	61.85	62.22	96.81	65.19	51.44	63.22
	DT	64.14	64.79	95.05	61.25	51.76	65.19
	RF	80.64	78.62	96.36	79.92	68.09	79.04
	MSVM	84.25	78.53	98.46	80.35	70.56	81.16
	AdaBoost	89.11	89.49	96.81	89.05	85.26	90.11
	Autoencoder	93.20	97.26	96.67	96.99	91.85	95.99
GWO	KNN	64.04	63.35	95.91	64.22	51.85	63.32
	DT	65.12	61.66	96.89	60.64	49.96	60.58
	RF	76.41	78.87	96.90	78.60	68.77	78.19
	MSVM	85.13	77.57	87.52	78.84	71.15	82.36
	AdaBoost	87.96	90.93	90.04	90.41	85.97	90.24
	Autoencoder	94.21	95.38	95.17	93.03	94.24	96.75
ACO	KNN	62.08	61.94	98.07	66.38	53.13	64.40
	DT	64.52	62.57	98.71	64.24	48.70	62.38
	RF	77.47	75.93	97.69	75.74	72.08	76.11
	MSVM	74.53	73.17	97.01	81.05	69.72	89.29
	AdaBoost	90.27	89.47	96.57	92.31	84.89	91.65
	Autoencoder	94.81	96	96.32	94.23	95.66	97.06
ABC	KNN	65.29	65.70	99.09	66.70	54.73	66.28
	DT	64.52	64.58	97.46	64	53.68	63.38
	RF	80.99	79.39	97.22	77.92	70.67	80.19
	MSVM	86.50	78.73	97.85	82.19	72.96	80.71
	AdaBoost	90.88	92.25	98.95	91.20	85.90	91.88
	Autoencoder	95.36	96.49	97.13	95.66	93.80	96.07
MABC	KNN	66.70	66.71	99.85	67.24	55.59	67.31
	DT	65.80	65.84	99.84	65.47	54.42	65.55
	RF	81.02	81.07	99.91	80.80	72.19	80.86
	MSVM	88.98	79.02	99.72	82.90	74.87	82.98
	AdaBoost	92.61	92.71	99.97	92.86	88.24	92.89
	Autoencoder	*98.73*	*97.89*	*99.99*	*97.78*	*96.33*	*97.79*

Fig. 6 Graphical presentation of MABC-autoencoder model on IIT Delhi v1.0 iris dataset with different feature selection algorithms

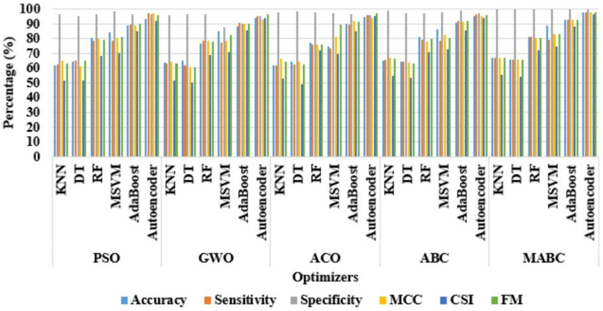

(ACO), ABC and MABC optimizers in terms of accuracy, sensitivity, specificity, MCC, CSI and FM index. PSO searches for an optimal solution using an objective function that is independent of gradient or any differential form. GWO is based on a large-scale search method positioned on optimal samples. ABC is a graphical approach to find good paths using probabilistic technique. By analyzing Table 2, the combination, MABC with autoencoder attained high accuracy of 98.73%, sensitivity of 97.89%, MCC of 97.78%, specificity of 99.99%, CSI of 96.33% and FM index of 97.79% in iris recognition. MABC-autoencoder with hybrid features showed a minimum of 2.37%, and a maximum of 35.8% accuracy improvement in iris recognition compared to other feature selection algorithms, and classification techniques. The graphical presentation of MABC-autoencoder model on IIT Delhi v1.0 iris dataset with different feature selection algorithms is shown in Fig. 6.

Table 3 Performance evaluation of MABC-autoencoder model on CASIA-Iris dataset with different feature extraction and classification techniques

Without feature selection

Features	*Classifiers*	*Accuracy (%)*	*Sensitivity (%)*	*Specificity (%)*	*MCC (%)*	*CSI (%)*	*FM (%)*
GLCM	KNN	48.23	45.80	39.50	63.79	27.51	44.13
	DT	40.62	48.09	64.62	51.90	37.80	51.74
	RF	56.16	46.86	59.41	54.71	55.49	54
	MSVM	52.91	46.09	68.28	60.61	56.80	64.46
	AdaBoost	43.98	59.96	58.52	52.51	29.68	48.60
	Autoencoder	59.94	79.76	74.06	83.81	53.83	75.27
LBP	KNN	45.77	42.31	38.59	60.98	24.37	43.29
	DT	32.53	43.62	58.78	48.60	31.01	48.79
	RF	53.48	45.37	50.60	49.13	51.40	52.98
	MSVM	45.90	40.73	62.77	56.70	53.26	63.59
	AdaBoost	37.24	55.56	58.07	47.02	48.79	40.56
	Autoencoder	59.14	71.77	70.20	75.48	52.71	68.34
Gabor	KNN	58.12	51.98	45.82	69.07	28.94	50.08
	DT	43.67	51.29	65.74	57.82	46.87	57.01
	RF	64.50	52.83	67.10	61.18	62.62	57.98
	MSVM	53.14	46.41	77.43	67.90	67.58	67.95
	AdaBoost	52.16	62.69	63.94	64.46	54.73	53.42
	Autoencoder	62.26	80.12	81.26	91.70	61.79	75.32
DTCWT	KNN	61.13	59.69	43.47	80.17	39.87	59.91
	DT	49.88	54.24	71.64	57.74	51.39	57.36
	RF	66.70	49.21	60.70	65.85	68.82	62.15
	MSVM	56.66	51.03	69.48	61.96	60.92	77.51
	AdaBoost	53.93	61.95	64.96	55.17	61.85	79.75
	Autoencoder	73.79	89.13	79.52	89.46	63.18	91.03
Hybrid	KNN	61.77	58.68	75.22	57.55	48.66	61.51
	DT	62.90	61.02	87.23	54	49	57.95
	RF	74.57	71.53	94.58	72.01	67.62	73.59
	MSVM	82.83	87.57	90.72	73.80	77.30	87.42
	AdaBoost	83.93	87.28	89.02	86.23	80.50	90.09
	Autoencoder	90.57	89.27	95.77	95.14	88.63	94.46

Fig. 7 Graphical presentation of MABC-autoencoder model on CASIA-Iris dataset with different feature extraction and classification techniques

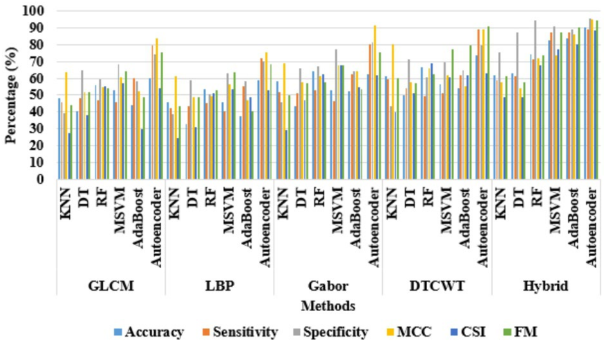

Table 4 Performance evaluation of MABC-autoencoder model on CASIA-Iris dataset with different feature selection algorithms

With feature selection

Optimizers	*Classifiers*	*Accuracy (%)*	*Sensitivity (%)*	*Specificity (%)*	*MCC (%)*	*CSI (%)*	*FM (%)*
PSO	KNN	60.60	61.83	98.32	66.24	50.75	64.10
	DT	58.73	66.57	93.20	63.57	52.32	62.34
	RF	76.46	84.11	90.28	79.98	67.06	82.02
	MSVM	76.60	79.10	90.35	79	63.06	75.09
	AdaBoost	88.09	90.55	90.69	83.58	85.31	89.14
	Autoencoder	90.58	93.53	97.74	94.83	90.82	91.26
GWO	KNN	68.10	63.12	68.42	72.04	51.52	64.04
	DT	71.13	71.85	95.59	61.74	52.69	68.22
	RF	86.53	81.54	86.12	83.87	70.34	81.88
	MSVM	85.77	83.95	81.53	86.76	77.08	82.68
	AdaBoost	95.58	95.45	94.82	96.81	90.06	96.46
	Autoencoder	93.69	98.07	93.31	99	95.87	97.71
ACO	KNN	59.25	66.08	75.47	69.41	58.53	64.74
	DT	62.41	70.45	93.13	65.56	55.47	65.83
	RF	79.69	80.96	94.42	77.46	69.55	83.44
	MSVM	83.02	76.84	81.41	82.52	67.07	78.66
	AdaBoost	93.69	94.59	95.62	90.14	85.84	90.01
	Autoencoder	94.73	95.37	98.10	95.36	94.52	96.85
ABC	KNN	62.57	68.91	62.87	72.93	53.64	70.75
	DT	68	68.63	71.27	66.09	53.95	72.98
	RF	84.22	80.64	80.52	85.41	69.76	81.34
	MSVM	85.02	82.92	91.27	84.28	70.64	88.87
	AdaBoost	96.79	90.56	91.04	92.68	86.86	92.94
	Autoencoder	96.65	98.51	93	97.55	95.26	94.89
MABC	KNN	62.19	68.92	64.45	69.42	58.67	66.31
	DT	66.35	70.81	96.29	69.23	56.67	66.17
	RF	82.73	84.36	97.98	81.16	72.91	83.62
	MSVM	84.22	80.64	90.52	85.41	69.76	81.34
	AdaBoost	94.10	97.09	97.72	91.20	88.78	90.80
	Autoencoder	*99.67*	*99.20*	*99.45*	*99.93*	*96.31*	*98.65*

5.2 Quantitative study on CASIA-Iris dataset

MABC-autoencoder model performance is tested on the CASIA-Iris dataset, which consists of 20,000 eye images. As seen in Table 3, the performance evaluation is carried out for individual feature extraction and traditional classification techniques in terms of accuracy, sensitivity, secificity, MCC, CSI and FM index. The combination, hybrid features with autoencoder classifier obtained a high accuracy of 90.57%, MCC of 95.14%, the sensitivity of 89.27%, specificity of 95.77%, CSI of 88.63%, and FM index of 94.46% on CASIA-Iris dataset. The obtained result is noteworthy in iris recognition related to comparative classifiers and individual feature extraction techniques on CASIA-Iris. The graphical presentation of proposed model on CASIA-Iris dataset with different feature extraction and classification techniques is specified in Fig. 7.

In Table 4, the performance is evaluated with optimization algorithms such as PSO, GWO, ACO, ABC, and MABC in terms of accuracy, sensitivity, specificity, MCC, CSI and FM index. As denoted in Table 4, MABC optimizer with autoencoder classifier attained higher accuracy of 99.67%, specificity of 99.45%, MCC of 99.93%, sensitivity of 99.20%, CSI of 96.31%, and FM index of 98.65% in iris recognition. Hence, MABC-autoencoder showed a minimum of 2.88%, and a maximum of 40.94% accuracy improvement in iris recognition on CASIA-Iris dataset. The graphical presentation of MABC-autoencoder model on CASIA-Iris dataset with different feature selection algorithms is shown in Fig. 8.

5.3 Comparative analysis

Tobji, et al. FMnet algorithm was based on MCNN and FCN [19]. The algorithm performance was tested on CASIA-Iris dataset in terms of accuracy. The experiment demonstrated that the algorithm achieved 95.63% of accuracy on CASIA-Iris dataset. Further, Jayanthi, et al. developed a deep learning model for accurate iris detection and recognition [20]. Initially, black hat filter, Gamma correction, and median filter were used to denoise raw eye images. Next, HCT technique was developed to localize iris regions, and R-CNN with Inception v2 technique was introduced for iris recognition. The simulation results showed that the deep learning model obtained 99.14% of accuracy on CASIA-Iris dataset. Jan and N. Min-Allah, developed an optimized coarse to fine method based on adaptive threshold to mark inner and outer boundaries in the eye images [24]. Fourier series was used to regularize noncircular iris contour and to mark reflections and eyelids in the polar form. In the resulting

Fig. 8 Graphical presentation of MABC-autoencoder model on CASIA-Iris dataset with different feature selection algorithms

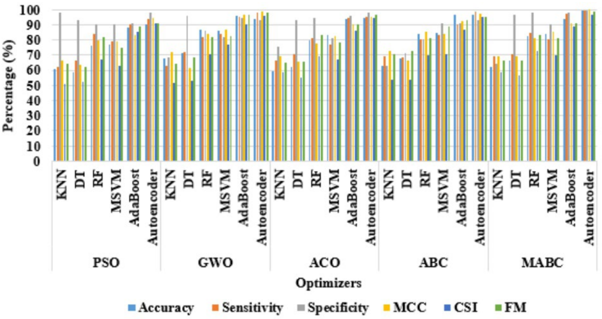

phase, developed model obtained 98% of accuracy in iris recognition on IIT Delhi v1.0 iris dataset. Jan, et al. used bilinear interpolation method and order static filter to preprocess input eye images [25]. The pupil's radius and center were extracted using geometry and centroid concepts, and then CHT and Fourier series were utilized to mark iris outer boundary regions and to refine coarse iris boundaries. The analysis showed that the presented model obtained 98.60% of accuracy on IIT Delhi v1.0 iris dataset. Compared to existing studies, the proposed MABC-autoencoder model obtained high accuracy of 98.73%, and 99.67% on IIT Delhi v1.0 iris dataset, and CASIA-Iris dataset, respectively. The comparative analysis between the existing and the proposed model is given in Table 5.

5.4 Discussion

Segmentation, feature selection and classification are the integral parts of proposed iris recognition model. Daugman's algorithm and CHT significantly segment the iris region from the collected images. MABC optimization algorithm is proposed to select the discriminative feature vectors from total extracted features that effectively decrease the execution time of the system and further the selected feature values are fed to autoencoder classifier for recognition. The proposed MABC-autoencoder model consumed 68.23 s and 49.52 s on CASIA-Iris and IIT Delhi v1.0 iris datasets to train and test the images. In Table 5, MABC-autoencoder model showed almost 0.13–0.73% improvement in accuracy on IIT Delhi v1.0 iris dataset compared to coarse to fine method-Fourier series [24] and CHT-Fourier series [25]. Similarly, the proposed MABC-autoencoder model showed almost 0.53–4.04% improvement in accuracy on CASIA-Iris dataset compared to fully and multi-scale CNN [19], and integrated deep learning model [20]. The experimental result confirmed that MABC-autoencoder model attained substantial performance under the conditions of occlusion, motion blur and defocus. Further, the execution time is minimum on both datasets as compared to related classifiers, and computational complexity is linear while using MABC optimizer.

6 Conclusion

A novel deep learning based integrated model named MABC-autoencoder model is proposed for accurate iris recognition. The model includes three major phases such as iris segmentation, feature selection and classification. Daugman's algorithm and CHT are developed to

Table 5 Comparative analysis between existing and the proposed model

Model	Dataset	Accuracy (%)
Fully and multi-scale CNN [19]	CASIA-Iris	95.63
Integrated deep learning model [20]	CASIA-Iris	99.14
Coarse to fine method-Fourier series [24]	IIT Delhi v1.0 iris	98
CHT-Fourier series [25]	IIT Delhi v1.0 iris	98.60
MABC-autoencoder model	*CASIA-Iris*	*99.67*
	IIT Delhi v1.0 iris	*98.73*

accurately segment the iris region from eye images. The developed algorithms obtained acceptable segmentation performance even under the conditions like occlusion, motion blur and defocus. Further, a MABC optimization algorithm is proposed to select discriminative feature vectors from the total features that effectively reduces the cause of "curse of dimensionality" issue, system complexity and execution time of the model. Lastly, the obtained discriminative features are given as the input to autoencoder classifier for iris recognition. In the experimental phase, MABC-autoencoder model achieved 99.67%, and 98.73% accuracy on CASIA-Iris, and IIT Delhi v1.0 iris datasets. Compared to existing classifiers and optimizers, the MABC-autoencoder model showed improved recognition performance in terms of FM index, MCC, accuracy, specificity, CSI, and sensitivity. Additionally, the computational complexity of MABC-autoencoder model is linear$O\left(n\right)$, where n states input size and O represents the order of magnitude. In future, an evolutionary based search algorithm can be included to identify an optimal set of feature vectors, and the recognition model could be evaluated under different environments and constraints.

References

1. Raja J, Gunasekaran K, Pitchai R (2019) Prognostic evaluation of multimodal biometric traits recognition based human face, finger print and iris images using ensembled SVM classifier. Cluster Comput 22(1):215–228
2. Nguyen K, Fookes C, Ross A, Sridharan S (2017) Iris recognition with off-the-shelf CNN features: A deep learning perspective. IEEE Access 6:18848–18855
3. Wang K, Kumar A (2019) Cross-spectral iris recognition using CNN and supervised discrete hashing. Pattern Recogn 86:85–98
4. Liu M, Zhou Z, Shang P, Xu D (2019) Fuzzified image enhancement for deep learning in iris recognition. IEEE Trans Fuzzy Syst 28(1):92–99
5. Jenadeleh M, Pedersen M, Saupe D (2020) Blind quality assessment of iris images acquired in visible light for biometric recognition, Sensors, vol.20, no.5, pp. 1308
6. Ahmadi N, Akbarizadeh G (2020) Iris tissue recognition based on GLDM feature extraction and hybrid MLPNN-ICA classifier. Neural Comput Appl 32(7):2267–2281
7. Arsalan M, Naqvi RA, Kim DS, Nguyen PH, Owais M, Park KR (2018) IrisDenseNet: Robust iris segmentation using densely connected fully convolutional networks in the images by visible light and near-infrared light camera sensors. Sensors 18(5):1501
8. Ohmaid H, Eddarouich S, Bourouhou A, Timouyas M (2020) Iris segmentation using a new unsupervised neural approach, IAES International Journal of Artificial Intelligence, vol. 9, no.1, pp. 58
9. Lin YN, Hsieh TY, Huang JJ, Yang CY, Shen VR, Bui HH (2020) Fast Iris localization using Haar-like features and AdaBoost algorithm. Multimedia Tools and Applications 79(45):34339–34362
10. Alam MM, Khan MAR, Salehin ZU, Uddin M, Soheli SJ, Khan TZ (2020) Combined PCA-Daugman Method: An Efficient Technique for Face and Iris Recognition, Journal of Advances in Mathematics and Computer Science, pp. 34–44
11. Ismail S, Ali FHM, Aljunid SA (2020) Reducing intra-class variations of deformed iris recognition system, International Journal of Advanced Trends in Computer Science and Engineering, vol. 9, no.1.3
12. Dua M, Gupta R, Khari M, Crespo RG (2019) Biometric iris recognition using radial basis function neural network. Soft Comput 23(22):11801–11815
13. Nithya AA, Lakshmi C (2019) Enhancing iris recognition framework using feature selection and BPNN. Cluster Comput 22(5):12363–12372
14. Ahmadi N, Nilashi M, Samad S, Rashid TA, Ahmadi H (2019) An intelligent method for iris recognition using supervised machine learning techniques, Optics & Laser Technology, vol. 120, pp. 105701
15. Ahmadi N, Akbarizadeh G (2018) Hybrid robust iris recognition approach using iris image pre-processing, two-dimensional Gabor features and multi-layer perceptron neural network/PSO. IET Biom 7(2):153–162
16. Adamović S, Miškovic V, Maček N, Milosavljević M, Šarac M, Saračević M, Gnjatović M (2020) An efficient novel approach for iris recognition based on stylometric features and machine learning techniques. Future Generation Computer Systems 107:144–157

17. Shuai L, Yuanning L, Xiaodong Z, Guang H, Jingwei C, Qixian Z, Zukang W, Xinlong L, Chaoqun W (2020) Multi-source feature fusion and entropy feature lightweight neural network for constrained multi-state heterogeneous iris recognition. IEEE Access 8:53321–53345
18. Chen Y, Wu C, Wang Y (2020) T-center: A novel feature extraction approach towards large-scale iris recognition. IEEE Access 8:32365–32375
19. Tobji R, Di W, Ayoub N (2019) FMnet: iris segmentation and recognition by using fully and multi-scale CNN for biometric security, Applied Sciences, vol.9, no.10, pp. 2042
20. Jayanthi J, Lydia EL, Krishnaraj N, Jayasankar T, Babu RL, Suji RA (2020) An effective deep learning features based integrated framework for iris detection and recognition, Journal of Ambient Intelligence and Humanized Computing, pp. 1–11
21. Vyas R, Kanumuri T, Sheoran G, Dubey P (2019) Efficient iris recognition through curvelet transform and polynomial fitting, Optik, vol.185, pp. 859–867
22. Juneja K, Rana C (2021) Compression-Robust and Fuzzy-Based Feature-Fusion Model for Optimizing the Iris Recognition. Wireless Pers Commun 116(1):267–300
23. Kumar MR, Arthi K (2020) An effective non-cooperative iris recognition system using hierarchical collaborative representation-based classification. J Supercomputing 76(8):5835–5848
24. Jan F, Min-Allah N (2020) An effective iris segmentation scheme for noisy images. Biocybernetics and Biomedical Engineering 40(3):1064–1080
25. Jan F, Min-Allah N, Agha S, Usman I, Khan I (2021) A robust iris localization scheme for the iris recognition. Multimedia Tools and Applications 80(3):4579–4605
26. Singh G, Singh RK, Saha R, Agarwal N (2020) IWT based iris recognition for image authentication. Procedia Comput Sci 171:1868–1876
27. Ignat A, Păvăloi I (2020) Experiments on iris recognition using SURF descriptors, texture and a repetitive method. Procedia Comput Sci 176:175–184
28. IITD Iris Dataset, url: https://www4.comp.polyu.edu.hk/~csajaykr/IITD/Database_Iris.htm
29. CASIA Dataset, url: https://hycasia.github.io/dataset/casia-irisv4/
30. Yang P, Zhang F, Yang G (2018) Fusing DTCWT and LBP based features for rotation, illumination and scale invariant texture classification. IEEE access 6:13336–13349
31. Muthukumar A, Kavipriya A (2019) A biometric system based on Gabor feature extraction with SVM classifier for Finger-Knuckle-Print. Pattern Recognit Lett 125:150–156
32. Kaplan K, Kaya Y, Kuncan M, Ertunç HM (2020) Brain tumor classification using modified local binary patterns (LBP) feature extraction methods, Medical hypotheses, vol. 139, pp. 109696
33. Garg M, Dhiman G (2020) A novel content-based image retrieval approach for classification using GLCM features and texture fused LBP variants, Neural Computing and Applications, pp. 1–18
34. Zhou J, Gao L, Yao X, Chan FT, Zhang J, Li X, Lin Y (2019) A decomposition and statistical learning based many-objective artificial bee colony optimizer. Inf Sci 496:82–108
35. Karaboga D, Ozturk C (2011) A novel clustering approach: Artificial Bee Colony (ABC) algorithm. Appl Soft Comput 11(1):652–657
36. Zhou P, Han J, Cheng G, Zhang B (2019) Learning compact and discriminative stacked autoencoder for hyperspectral image classification. IEEE Trans Geosci Remote Sens 57(7):4823–4833

Publisher's Note Springer Nature remains neutral with regard to jurisdictional claims in published maps and institutional affiliations.